nature portfolio

https://doi.org/10.1038/s41550-021-01375-3

Supplementary information

Haze evolution in temperate exoplanet atmospheres through surface energy measurements

In the format provided by the authors and unedited

Haze Evolution in Temperate Exoplanet Atmospheres Through Surface Energy Measurements

Xinting Yu*[,1], Chao He[2], Xi Zhang[1], Sarah M. Hörst[2], Austin H. Dymont[3], Patricia McGuiggan[4], Julianne I. Moses[5], Nikole K. Lewis[6], Jonathan J. Fortney[7], Peter Gao[7], Eliza M.-R. Kempton[8], Sarah E. Moran[2], Caroline V. Morley[9], Diana Powell[7], Jeff A. Valenti[10], Véronique Vuitton[11]

[1]Department of Earth and Planetary Sciences, University of California Santa Cruz, 1156 High Street, Santa Cruz, California 95064, USA
[2]Department of Earth and Planetary Sciences, Johns Hopkins University, 3400 N. Charles Street, Baltimore, Maryland 21218, USA
[3]Department of Physics, University of California Santa Cruz, 1156 High Street, Santa Cruz, California 95064, USA
[4]Department of Materials Science and Engineering, Johns Hopkins University, 3400 N. Charles Street, Baltimore, Maryland 21218, USA
[5]Space Science Institute, Boulder, CO 80301, USA
[6]Department of Astronomy and Carl Sagan Institute, Cornell University, 122 Sciences Drive, Ithaca, NY 14853, USA
[7]Department of Astronomy and Astrophysics, University of California Santa Cruz, 1156 High Street, Santa Cruz, California 95064, USA
[8]Department of Astronomy, University of Maryland, College Park, MD 20742, USA
[9]Department of Astronomy, The University of Texas at Austin, Austin, TX 78712, USA
[10]Space Telescope Science Institute, Baltimore, MD 21218, USA
[11]University Grenoble Alpes, CNRS, CNES, IPAG, F-38000 Grenoble, France

April 8, 2021

*Email: xintingyu@ucsc.edu

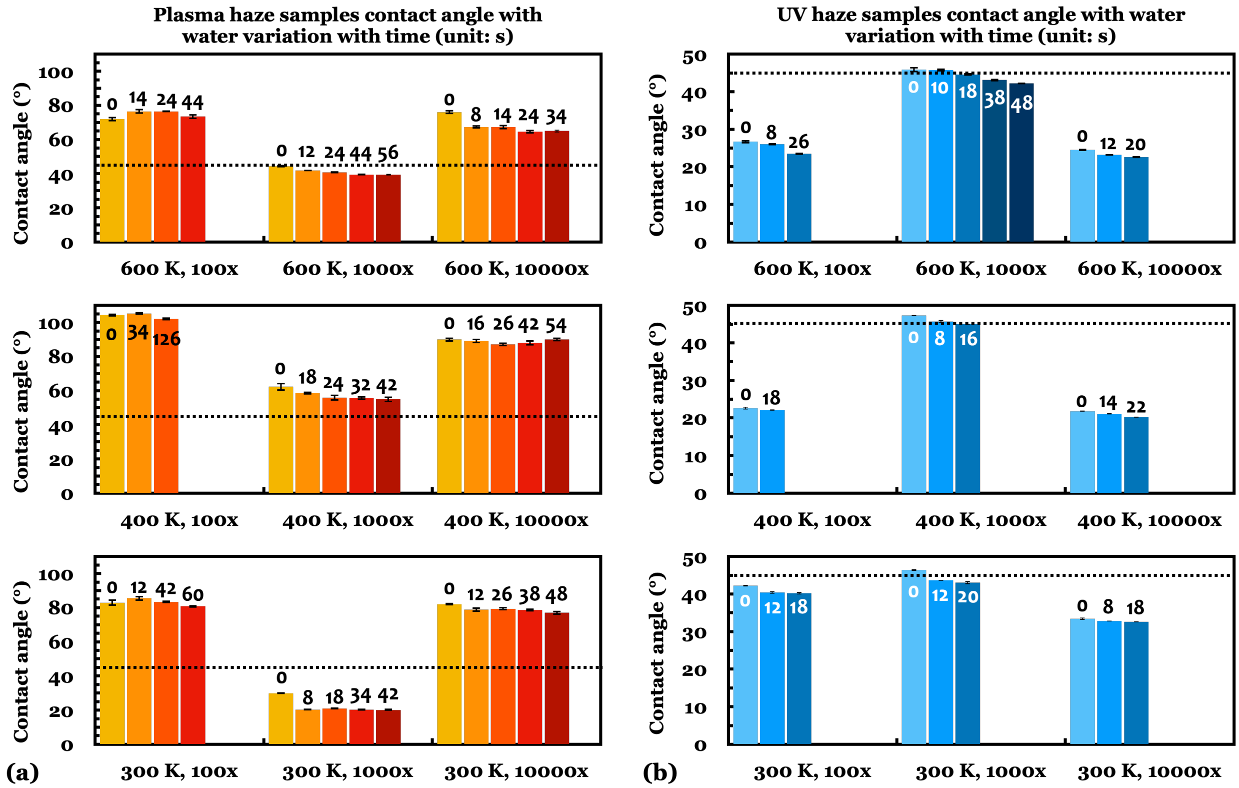

Supplementary Figure 1: **Variation of the measured mean contact angles with time between the haze samples and liquid water.** (a) Contact angle variation for the plasma haze samples. (b) Contact angle variation for the UV haze samples. All marked times are in seconds. All contact angles was measured through circle fitting. The error bars represent 1-σ s.d. measurement uncertainties from the fitting algorithm.

References

[1] Lifshitz, E. M. & Hamermesh, M. The theory of molecular attractive forces between solids. In Perspectives in Theoretical Physics (Pergamon, 1992).

[2] Israelachvili, J. N. Intermolecular and surface forces (Academic Press, 2011).

Supplementary Table 1: **Measured mean contact angle values between the test liquids and the plasma exoplanet tholin samples.** All numbers have units of degrees. The contact angle was measured through both circle fitting and ellipse fitting. The 1-σ s.d. measurement uncertainties for each fitting algorithms are also recorded.

Liquid	600 K, 100×				600 K, 1000×				600 K, 10000×			
	Circle	SD	Ellipse	SD	Circle	SD	Ellipse	SD	Circle	SD	Ellipse	SD
Water	78.4	1.6	74.8	3.9	45.4	1.1	44.8	1.8	82.4	4.5	81.1	5.2
Diiodomethane	44.3	2.3	41.9	2.7	48.2	1.4	46.9	3.2	58.7	4.4	57.9	6.0
Liquid	400 K, 100×				400 K, 1000×				400 K, 10000×			
	Circle	SD	Ellipse	SD	Circle	SD	Ellipse	SD	Circle	SD	Ellipse	SD
Water	102.7	3.7	101.9	3.1	64.7	0.7	62.0	1.8	91.5	1.7	91.1	2.8
Diiodomethane	60.5	1.7	61.0	2.0	49.6	4.5	49.4	4.5	48.3	2.3	50.3	2.9
Liquid	300 K, 100×				300 K, 1000×				300 K, 10000×			
	Circle	SD	Ellipse	SD	Circle	SD	Ellipse	SD	Circle	SD	Ellipse	SD
Water	86.7	1.4	82.9	1.9	32.5	2.6	33.0	3.0	85.3	3.3	83.1	4.3
Diiodomethane	53.1	5.0	49.7	3.5	50.7	0.6	51.1	2.3	56.8	2.0	54.1	3.6

Supplementary Table 2: **Measured mean contact angle values between the test liquids and the UV exoplanet tholin samples.** All numbers have units of degrees. The contact angle was measured through both circle fitting and ellipse fitting. The 1-σ s.d. measurement uncertainties for each fitting algorithms are also recorded.

Liquid	600 K, 100×				600 K, 1000×				600 K, 10000×			
	Circle	SD	Ellipse	SD	Circle	SD	Ellipse	SD	Circle	SD	Ellipse	SD
Water	23.6	2.5	24.6	3.4	46.8	3.2	45.9	3.7	23.7	1.5	25.1	2.9
Diiodomethane	51.2	0.8	49.9	2.8	59.4	0.8	57.4	2.4	43.9	1.4	42.4	1.9
Liquid	400 K, 100×				400 K, 1000×				400 K, 10000×			
	Circle	SD	Ellipse	SD	Circle	SD	Ellipse	SD	Circle	SD	Ellipse	SD
Water	28.5	6.2	28.7	5.8	49.2	2.5	48.2	2.0	20.6	0.7	21.4	1.5
Diiodomethane	40.1	2.6	38.9	2.8	52.6	3.1	52.0	3.1	44.2	2.1	42.6	3.3
Liquid	300 K, 100×				300 K, 1000×				300 K, 10000×			
	Circle	SD	Ellipse	SD	Circle	SD	Ellipse	SD	Circle	SD	Ellipse	SD
Water	40.6	1.0	38.3	1.8	40.9	5.6	39.6	5.3	36.1	3.2	35.4	2.6
Diiodomethane	47.9	1.6	47.1	2.9	60.6	2.3	58.0	2.5	46.3	1.4	44.4	2.1

Supplementary Table 3: **The derived mean surface energy values of the cold plasma exoplanet haze samples.** The surface energy values are derived with the OWRK two-liquid method using the circle fitting contact angles in Supplementary Table 1. The total surface energy, γ_s^{tot}, can be partitioned into a dispersive component, γ_s^d, and a polar component, γ_s^p. All numbers have units of mJ/m^2. The error ranges shown are 1-σ s.d. uncertainties calculated through propagation of error.

600 K, 100×				600 K, 1000×				600 K, 10000×			
γ_s^{tot}		SD		γ_s^{tot}		SD		γ_s^{tot}		SD	
41.9		1.3		58.3		0.9		34.3		2.9	
γ_s^d	γ_s^p	SD^d	SD^p	γ_s^d	γ_s^p	SD^d	SD^p	γ_s^d	γ_s^p	SD^d	SD^p
37.4	4.5	0.9	1.0	35.3	23.0	0.6	0.8	29.3	5.0	1.9	2.6
400 K, 100×				400 K, 1000×				400 K, 10000×			
γ_s^{tot}		SD		γ_s^{tot}		SD		γ_s^{tot}		SD	
28.5		2.1		46.3		1.8		36.4		1.3	
γ_s^d	γ_s^p	SD^d	SD^p	γ_s^d	γ_s^p	SD^d	SD^p	γ_s^d	γ_s^p	SD^d	SD^p
28.3	0.2	0.7	2.1	34.5	11.8	1.8	1.2	35.2	1.2	0.9	1.1
300 K, 100×				300 K, 1000×				300 K, 10000×			
γ_s^{tot}		SD		γ_s^{tot}		SD		γ_s^{tot}		SD	
35.3		1.9		65.1		1.3		34.0		1.9	
γ_s^d	γ_s^p	SD^d	SD^p	γ_s^d	γ_s^p	SD^d	SD^p	γ_s^d	γ_s^p	SD^d	SD^p
32.5	2.8	2.1	1.3	33.9	31.2	0.2	1.3	30.4	3.6	0.8	1.8

Supplementary Table 4: **The derived mean surface energy values of the UV exoplanet haze samples.** The surface energy values are derived with the OWRK two-liquid method using the circle fitting contact angles in Supplementary Table 2. The total surface energy, γ_s^{tot}, can be partitioned into a dispersive component, γ_s^d, and a polar component, γ_s^p. All numbers have units of mJ/m^2. The error ranges shown are 1-σ s.d. uncertainties calculated through propagation of error.

600 K, 100×				600 K, 1000×				600 K, 10000×			
γ_s^{tot}		SD		γ_s^{tot}		SD		γ_s^{tot}		SD	
69.3		1.1		54.6		1.9		70.7		0.9	
γ_s^d	γ_s^p	SD^d	SD^p	γ_s^d	γ_s^p	SD^d	SD^p	γ_s^d	γ_s^p	SD^d	SD^p
33.6	35.7	0.3	1.0	28.9	25.7	0.3	1.9	37.6	33.1	0.5	0.8
400 K, 100×				**400 K, 1000×**				**400 K, 10000×**			
γ_s^{tot}		SD		γ_s^{tot}		SD		γ_s^{tot}		SD	
69.5		3.1		54.7		2.0		71.8		1.0	
γ_s^d	γ_s^p	SD^d	SD^p	γ_s^d	γ_s^p	SD^d	SD^p	γ_s^d	γ_s^p	SD^d	SD^p
39.6	29.9	0.9	3.0	32.8	21.9	1.3	1.8	37.4	34.4	0.8	0.7
300 K, 100×				**300 K, 1000×**				**300 K, 10000×**			
γ_s^{tot}		SD		γ_s^{tot}		SD		γ_s^{tot}		SD	
61.2		0.9		58.2		3.3		64.1		1.9	
γ_s^d	γ_s^p	SD^d	SD^p	γ_s^d	γ_s^p	SD^d	SD^p	γ_s^d	γ_s^p	SD^d	SD^p
35.4	25.8	0.6	0.8	28.2	30.0	1.0	3.3	36.3	27.8	0.5	1.8

Supplementary Table 5: **Derived mean refractive indices of the haze samples in the visible wavelengths (n_{vis}).** The refractive indices are derived using the Liftshitz theory of van der Waals forces [1, 2]. The error ranges shown are 1-σ s.d. uncertainties calculated through propagation of error.

Plasma			UV		
600 K, 100×	600 K, 1000×	600 K, 10000×	600 K, 100×	600 K, 1000×	600 K, 10000×
1.53±0.04	1.64±0.05	1.47±0.04	1.72±0.05	1.62±0.05	1.73±0.06
400 K, 100×	400 K, 1000×	400 K, 10000×	400 K, 100×	400 K, 1000×	400 K, 10000×
1.42±0.03	1.56±0.04	1.48±0.04	1.72±0.06	1.62±0.05	1.73±0.06
300 K, 100×	300 K, 1000×	300 K, 10000×	300 K, 100×	300 K, 1000×	300 K, 10000×
1.47±0.04	1.69±0.05	1.47±0.04	1.66±0.05	1.64±0.05	1.68±0.05
Titan plasma: 1.71±0.06			Titan UV: 1.70±0.06		

Supplementary Table 6: **Measured mean contact angle values between the test liquids and substrates.** All numbers have units of degrees. The contact angle was measured through both circle fitting and ellipse fitting. The 1-σ s.d. measurement uncertainties for each fitting algorithms are also recorded.

Liquid	Quartz disc				Cleaved mica			
	Circle	SD	Ellipse	SD	Circle	SD	Ellipse	SD
Water	15.2	2.0	16.6	2.6	spread	n/a	spread	n/a
Diiodomethane	36.8	1.0	39.3	1.9	38.8	1.5	39.4	1.7

Supplementary Table 7: **The derived mean surface energy values of the substrates.** The surface energy values are derived with the OWRK two-liquid method using the circle fitting contact angles in Supplementary Table 6. The total surface energy, γ_s^{tot}, can be partitioned into a dispersive component, γ_s^d, and a polar component, γ_s^p. All numbers have units of mJ/m^2. The error ranges shown are 1-σ s.d. uncertainties through propagation of error.

Quartz disc				Mica disk			
γ_s^{tot}		SD		γ_s^{tot}		SD	
75.1		0.9		76.8		0.6	
γ_s^d	γ_s^p	SD^d	SD^p	γ_s^d	γ_s^p	SD^d	SD^p
41.2	33.9	0.3	0.6	40.2	36.6	0.5	0.5